

Pulse Propagation in End-Linked Poly(dimethylsiloxane) Networks

Maitreyee Sinha,^{*,†,‡} Burak Erman,[§] James E. Mark,[‡] Thomas H. Ridgway,[‡] and Howard E. Jackson[†]

Department of Physics, University of Cincinnati, Cincinnati, Ohio 45221-0011; Department of Chemistry, University of Cincinnati, Cincinnati, Ohio 45221-0172; and Department of Chemical and Biological Engineering, Koc University, Rumelifeneri Yolu, Sariyer 80910, Istanbul, Turkey

Received March 11, 2003

ABSTRACT: The speed of a propagating pulse in polymer networks is strongly influenced by their microscopic structure. The measurement of pulse velocity can be used to determine network parameters, including the molecular weight of the network between chemical cross-links (M_c) and physical entanglements (M_e). We report an experimental method for determining these network parameters from measurements of transverse velocity in stretched samples of well-defined polymer networks. We measured the transverse propagation speed in end-linked poly(dimethylsiloxane) networks under uniaxial tension as a function of the extension ratio, the degree of cross-linking, and the amount of swelling. To determine M_c and M_e from these measurements, we used the theory of elastic wave propagation and molecular models for the networks to relate network parameters to the wave velocity in deformed networks. We compare and contrast the values of network parameters obtained using this method with independent measurements of network characteristics from other measurement techniques.

I. Introduction

Extensive work using both standing waves and ultrasonic measurements on rubberlike polymers has been reported.^{1–3} These efforts have been directed largely toward studying the change in sound velocity with temperature and frequency or toward the determination of various bulk properties such as the modulus and hysteresis of networks. Here we report measurements carried out with a custom-built experimental apparatus that allows accurate measurement of the speed of a propagating transverse pulse in a uniaxially stretched network. We carried out measurements of transverse pulse velocity in stretched poly(dimethylsiloxane) (PDMS) networks with average molecular weights between cross-links ranging from 800 to 30 000 g/mol. We also measured effects of swelling and fillers on the transverse pulse velocity in these networks. We derive a set of equations using the theory of elastic wave propagation and molecular models of networks to relate the speed of a propagating longitudinal or transverse pulse to network parameters such as M_c and M_e . We have used the equations and our measurements of the transverse pulse speed to estimate values of M_c and M_e for the networks.

One advantage of choosing PDMS is that this elastomer, unlike natural rubber, does not undergo crystallization under deformation in the vicinity of room temperature. Such strain-induced crystallization would present a considerable complication, since the crystallites thus generated would of course affect propagation speeds in the network. The ability to accurately determine the molecular weight of such well-characterized networks from independent methods allows us to compare the values calculated from the pulse velocity

measurements using the proposed theoretical framework. The elastomers were prepared using an end-linking technique.⁴ The network chains therefore have the same distribution of lengths as the sample of un-cross-linked chains from which they were prepared. Molecular weights of the network chains determined from the pulse propagation data are compared with GPC measurements carried out on the un-cross-linked chains, and some issues regarding entanglement spacings are addressed. Of central importance is establishing the extent to which this approach can provide reliable information on network structure.

In the following section, we outline the theoretical framework used for interpreting the experimental data. We briefly review the main results from theory of elastic wave propagation (section II.1) and molecular models of networks (section II.2) to discuss the applicability of these theories for this experimental method. On the basis of these arguments, we derive the speed of a propagating pulse in a dry or swollen, uniaxially stretched polymer network. We present these new equations in section II.3 and explain how these can be used to determine M_c and M_e from experimentally measured pulse speeds.

In section III, we describe the experimental apparatus that we built to measure the transverse pulse speed in a uniaxially stretched polymer network. In section IV, we provide the main results from experiments carried out on PDMS networks with a wide range of molecular weights. We report how the transverse pulse velocity depends on the applied strain, the molecular weight of the network, and the amount of fillers. In section IV.4, we quantitatively determine the network parameters, M_c and M_e , using the equations for transverse pulses derived in section II.3. We compare these values with molecular weights determined independently from GPC measurements carried out on network chains prior to cross-linking. Finally, we report the effect of swelling on the pulse speed and confirm that the measured pulse speed is lower than the speed in a dry network at the same extension ratio.

[†] Department of Physics, University of Cincinnati.

[‡] Department of Chemistry, University of Cincinnati.

[§] Koc University.

[‡] Present address: GE Global Research Center, Niskayuna, NY 12309.

* To whom correspondence should be addressed: e-mail sinha@crd.ge.com.

II. Theoretical Framework

We wish to derive the relationship for pulse speeds measured by the experimental apparatus described in section III, in terms of the network parameters and the state of deformation of the network. The propagation of mechanical disturbances in an elastic body subject to a finite static state of deformation has been investigated theoretically by various authors.^{5–8} A particularly simple case is the study of acceleration waves in which a sharp disturbance propagates in the form of a singular surface.⁵ Such a surface may be produced, for example, by applying an impulsive stress to the boundary of the body. The two most common wave fronts result from the propagation of longitudinal and transverse states of stress. Truesdell⁵ gives a concise account of the phenomenon, according to which the speed of propagation of a pulse can be related to the state of stress acting on an elastic body.

A polymeric network consisting of relatively long chains between cross-links is a good example where essentially two types of elastic behavior may be observed depending on the time scale of the deformation and the amount of solvent in the network. At short times, an unswollen network behaves like an elastic solid. The so-called plateau modulus of the network remains constant over several decades of the frequency. In this case, the network exhibits *instantaneous* elasticity. As will be discussed in more detail below, the characteristic relaxation time of the stress at the molecular level in the network is much longer than the time required for a wave front to propagate a given distance of the order of molecular dimensions. The wave front thus propagates without appreciable relaxation of the material. The theory of elastic wave propagation is therefore safely applicable in this instantaneous elasticity regime.

In the other extreme, a highly swollen network may be regarded as a true elastic network for which the characteristic relaxation times have been shifted to very short time scales due to the predominance of the small molecule solvent in the medium. The time required for the chains to attain their equilibrium is now much shorter than the time required for a wave front to propagate a given distance and the theory of elastic wave propagation is again valid. Between these two limits, the propagating wave front sees a viscoelastic environment, and a theory of viscoelastic wave propagation is required.⁹

In these two limits where elastic wave propagation is applicable for pulse propagation in deformed polymer networks, we can use appropriate molecular models for elastomeric networks to derive equations relating the pulse speeds to network parameters. For the sake of completeness, we provide the equations relating pulse speeds to the stress tensor^{5,10} from the theory of elastic wave propagation in section II.1 and equations relating the stress tensor to the molecular constitution and the state of deformation of the network¹¹ in section II.2. We combine these theories to propose equations for determining M_c and M_e from experimentally measured pulse speeds. Propagation in the highly swollen state is expected to yield information on the topological structure of the network whereas that in the dry state is related to the plateau modulus.

II.1. Propagation of a Pulse in an Elastic Body.

Choosing the propagating surface to move along the x_1 axis leads to explicit relations between the wave speeds and the state of stress (t) and strain (λ).¹⁰ The speed of

the longitudinal and transverse pulses is given by U_{11} and U_{12} , respectively⁵

$$\rho U_{11}^2 = \frac{\partial t_1}{\partial \ln \lambda_1} \quad (1)$$

$$\frac{\rho U_{12}^2}{\lambda_1^2} = \frac{t_1 - t_2}{\lambda_1^2 - \lambda_2^2} \quad (2)$$

Here t_1 and t_2 are the principal components of the Cauchy stress tensor or the true stress, along x_1 and x_2 , respectively.

Equations 1 and 2 are elegant and exact expressions for the wave speeds in an elastic body subject to a finite state of deformation. To use these equations to determine structural parameters of a deformed elastomeric network from experimentally measured wave speeds, the speeds U_{11} and U_{12} have to be expressed as a function of network parameters. For amorphous elastomeric networks, we will show how the well-established molecular models of networks allow us to derive these relations by providing the relationship of stress to deformation precisely in terms of molecular parameters.

II.2. Molecular Structure, Elastic Free Energy, and Relaxation Mechanisms of the Network. The molecular structure of a real network may conveniently be described in terms of the perfect unimodal network.¹¹ The latter consists of ν linear chains and μ junctions of functionality ϕ .¹² We associate the plateau region with the affine network model and the fully relaxed state with the phantom network model. The apparently fictitious phantom model of the network may be approached relatively closely if the already formed network is highly swollen with a nonvolatile solvent. At the extreme limit of phantom behavior, the elastic free energy per unit volume, ΔA , of the phantom network is expressed as¹²

$$\Delta A_{ph} = \frac{1}{2} \left(1 - \frac{2}{\phi} \right) \frac{\rho_d R T}{M_c} (v_{20}^{2/3} / v_2^{1/3}) (\alpha_1^2 + \alpha_2^2 + \alpha_3^2 - 3) \quad (3)$$

where T is the temperature, ρ_d is the density of the dry network, R is the gas constant, and M_c is the average molecular weight of the chains between junctions. For isotropic swelling, the measure of deformation is described by the stretch ratio, α , defined as

$$\alpha = L/L_i = (v_2/v_{20})^{1/3} \lambda \quad (4)$$

where L_i is the swollen undistorted length of the sample; v_2 and v_{20} are the volume fractions of the polymer in the deformed and undeformed states, respectively.

Contributions to the elastic free energy at higher values of v_2 and in the dry state result from the intermolecular interactions along the contours of the chains,^{13–15} and the expression for the elastic free energy departs significantly from that given by eq 3. The appearance of intermolecular interactions shifts the characteristic relaxation times of the network to much longer time scales. At sufficiently high frequencies, the network resides within the plateau region of instantaneous elasticity where a fictitious network may be considered with discrete entanglements playing the role of tetrafunctional cross-links. The cross-links may be assumed to deform affinely with macroscopic deforma-

tion.¹⁶ Denoting the average molecular weight of chains between entanglements by M_e , the following elastic free energy, valid at high frequencies, may be introduced

$$\Delta A_{pl} = \frac{1}{2} \frac{\rho RT}{M_e} (\alpha_1^2 + \alpha_2^2 + \alpha_3^2 - 3) \quad (5)$$

where the subscript pl indicates that the expression is valid in the plateau region.

The relaxation of uniaxial stress in a dry network stretched suddenly to a fixed length gives important information about the dominant relaxation times of the network. The relaxation behavior of the modulus may be approximated by the well-known Mooney–Rivlin plot with time-dependent coefficients $C_1(t)$ and $C_2(t)$

$$\text{modulus} \equiv t_1 v_2^{1/3} / (\alpha^2 - 1/\alpha) = C_1(t) + C_2(t)/\alpha \quad (6)$$

where α is the extension ratio in uniaxial deformation. Previous work^{17–19} on 1,2-polybutadiene,¹⁷ poly(isoprene),¹⁸ poly(dimethylsiloxane), and poly(ethyl acrylate)¹⁹ showed that at short time scales the modulus is close to the plateau modulus and does not depend on the degree of deformation; i.e., $C_2(t)$ in eq 6 is small and $C_1(t)$ is large. As time progresses, $C_1(t)$ decreases and $C_2(t)$ increases. At longer times, this behavior reverses itself, and $C_1(t)$ stops relaxing while $C_2(t)$ continues relaxing until the equilibrium Mooney–Rivlin plot is obtained. A highly swollen network may be approximated with a modulus where $C_2(t)$ is approximately zero, i.e., the modulus is independent of deformation, like that in the plateau modulus. In the present analysis, only the two extreme cases will be considered, the short time plateau and the long time equilibrium behavior, for both of which the moduli are independent of deformation. It is worth noting that the short-time behavior may be represented by the affine network and the long time behavior by the phantom network models of elasticity.

The stress may be related to the stored energy through the thermodynamic expression

$$t_i = \lambda_i \left(\frac{\partial \Delta A}{\partial \lambda_i} \right)_{T,V} \quad (7)$$

Substituting eqs 3 and 5 into eq 7 leads to¹¹

$$t_{1,ph} = \left(1 - \frac{2}{\phi} \right) \frac{\rho_d RT}{M_c} (v_{20}^{2/3} / v_2^{1/3}) (\alpha^2 - 1/\alpha) \quad (8)$$

$$t_{1,ph} = \frac{\rho_d RT}{M_c} (\alpha^2 - 1/\alpha)$$

In eq 8, v_2 is equated to unity inasmuch as only the dry network is of interest in the plateau region. Substituting eq 8 into eq 6 leads to the well-known expressions for the modulus of the network in the equilibrium and instantaneous elasticity regimes.^{11,16}

II.3. Speeds of Propagation of Longitudinal and Transverse Pulses in Networks under Uniaxial Tension or Compression. In sections II.1 and II.2 we reviewed results from theory of elastic wave propagation and the classic phantom and affine molecular models for networks to establish the two types of elastic behavior where this theoretical treatment will be valid, depending on the time scale of the deformation and the amount of solvent in the network. We now combine the

respective expressions for the stress with eqs 1 and 2 to obtain the speed of the longitudinal and transverse pulses (U_{11} and U_{12}).

$$U_{11,pl}^2 = \frac{RT}{M_e} \left(2\alpha^2 + \frac{1}{\alpha} \right) \quad (9)$$

$$U_{12,pl}^2 = \frac{RT}{M_e} \alpha^2 \quad (10)$$

$$U_{11,ph}^2 = \left(1 - \frac{2}{\phi} \right) \frac{RT}{M_c} (v_{20}/v_2)^{2/3} \left(2\alpha^2 + \frac{1}{\alpha} \right) \quad (11)$$

$$U_{12,ph}^2 = \left(1 - \frac{2}{\phi} \right) \frac{RT}{M_c} (v_{20}/v_2)^{2/3} \alpha^2 \quad (12)$$

where $\alpha = (v_{20}/v_2)^{2/3} \lambda$ and $\lambda = L/L_0$.

We propose that this new set of equations can be used to determine network parameters such as M_c and M_e from experimentally measured values of pulse speeds in stretched networks using the apparatus described in section III. The phantom modulus of ordinary networks with relatively long chains such as 10⁴ g/mol between cross-links is of the order of 0.1 MPa. Substituting this value of the molecular weight into eq 9, the speed of a longitudinal pulse for an unstretched tetrafunctional network with $v_{20}/v_2 = 1$ is obtained to be about 20 m/s. The value of v_2 for a network to reach the phantom state lies in general in the range of 0.1–0.2.¹¹ If the network is formed in the highly swollen state, the ratio v_{20}/v_2 will equal approximately unity. Thus, the calculated speed of 20 m/s for the longitudinal pulse may be regarded as a lower bound. At this speed, the longitudinal pulse induces a dilatational effect as it sweeps through the medium. However, this effect will not cause an appreciable motion of the solvent relative to the network. This can easily be seen by considering the characteristic times of diffusion of solvent into a swollen network that is of the order of 10^{–7} cm²/s.²⁰ If one assumes the thickness of the propagating surface to be of the order of a millimeter, the characteristic time for the solvent to squeeze out of this region is of the order of 10 s, while the time required for the wave to sweep through this distance is 5 × 10^{–7} s. Thus, the polymer–solvent system will move together in the course of the propagation of the pulse. In the case of a transverse pulse, the motion of the solvent relative to the polymer will not be of any consequence because transverse disturbances propagate through isovolumetric deformations.

The speed of a transverse pulse for the undeformed network considered above is calculated to be about 11 m/s. Thus, by measuring the speed at a known value of strain, this theoretical description will allow us to determine directly M_c and M_e for polymer networks. This analysis rests on the closeness of the constitutive state of the network to the elastic state. This will depend on the relaxation time of the chains in the network, the degree of entanglement and cross-linking of the chains, the amount of solvent in the network, the frequency of deformation, etc. Thus, depending on these various parameters, networks will exhibit different elastic regimes. When the propagating pulse probes a time varying environment where the molecules may still be rearranging in response to the mechanical disturbance, this theoretical treatment will no longer apply. Thus,

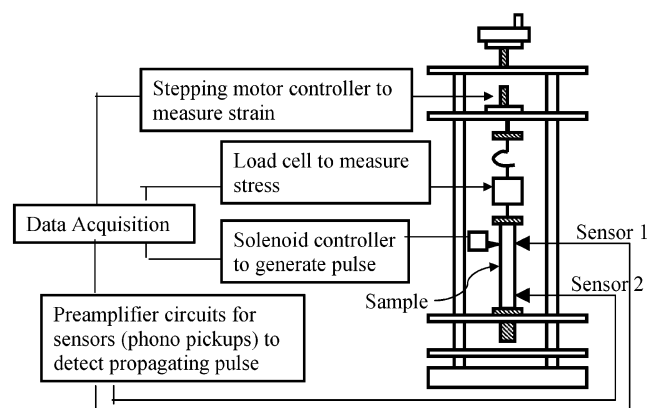


Figure 1. A schematic of the experimental arrangement showing the polymer strip clamped at two ends. The stepping motor controls the level of strain, the force gauge measures the stress in the network, the solenoid controls the excitation/pulse generation, and the sensors record the amplitude information as the pulse propagates.

deviations from these predictions will provide an indication of viscoelastic effects in the material.

III. Experimental Section

We designed and built a working apparatus for measuring the transverse pulse speed as a function of strain. As can be seen in the schematic of the apparatus in Figure 1, the sample was mounted between two clamps in the stress-strain apparatus with the upper clamp attached to a movable force gauge. We used a stepping motor controller to determine the extension of the sample. It was calibrated using a cathetometer. The smallest step size by which we can strain the sample is 0.001 in. The difference in extension ratios between values measured by the stepper motor/software extension values and those measured with the cathetometer was less than 1% over the range studied and was at the limit of resolution of the cathetometer. At a fixed level of strain, the stress in the network was measured using a load cell. The load cell was calibrated using known weights, and the error was about 0.1%. This allowed us to measure the stress-strain level in the network simultaneously with the acoustic experiments.

The pulse propagation experiments were carried out at a fixed level of strain. The excitation was provided by a computer-controlled solenoid valve, which used a thin high-pressure jet of argon to impart momentum to a small spherical pellet with 1/16 in. diameter to generate a transverse pulse. To detect the propagating pulse at the two ends of the sample, two phonograph pickups were placed in contact with the sample. The pickups were placed in contact with the flat face of the sample, opposite to the face on which the pellets were incident. Figure 2 shows a transverse pulse propagating through a PDMS network ($M_n = 17\,600$ g/mol). The signals detected by the phonograph pickups at the beginning and end of the sample (sensors 1 and 2, respectively) show the pulse amplitude as a function of time. The speed of the pulse can be obtained directly from the time difference between the two peaks.

We carried out pulse propagation experiments on end-linked PDMS for a wide range of number-averaged molecular weights between 800 and 30 000 g/mol. In our experiments we used end-linked hydroxyl-terminated PDMS with tetraethoxysilane (TEOS) and 0.8 wt % of the catalyst stannous octoate (STO) to form a tetrafunctional network.⁴ The networks were prepared in bulk with small amounts of toluene to facilitate mixing. Prior to network formation, gel permeation chromatography (GPC) experiments were carried out on the PDMS liquids to determine the molecular weight distributions. The molecular weights M_n , M_w and the polydispersity index (M_w/M_n) were determined using GPC data on 11 polystyrene standards and the Mark-Houwink constants for PDMS.²¹ The polydispersity indices were typically low with average values

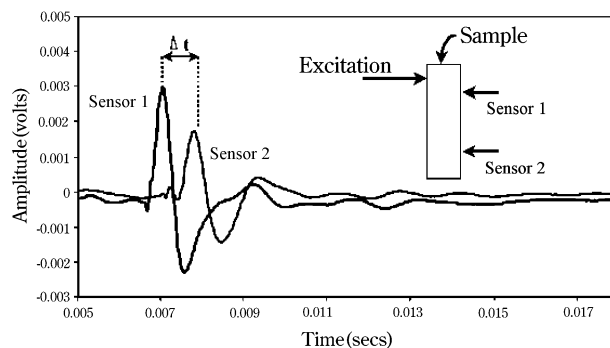


Figure 2. Transverse pulse propagation in PDMS network with $M_n = 17\,600$ g/mol at a fixed level of strain. The two pulse forms correspond to the signals detected by the two sensors placed at a known distance apart. From the time difference the speed of the pulse can be calculated.

of 1.4. Since an end-linking process was used to form the networks, the average molecular weight distribution between cross-links was the same as the molecular weight distribution of the un-cross-linked PDMS liquids from which they were prepared.

To remove any excess catalyst or un-cross-linked polymer, each cross-linked sheet was first weighed and then extracted at room temperature in toluene for 3 days, replacing the solvent every 24 h. The sample was weighed at the end of the swelling process. After the networks were extracted, they were deswollen in a series of toluene-methanol mixtures of increasing methanol content. The sample was then air-dried until the weight became constant. The total amount of material thus removed ranged from 2% to about 7%. The networks prepared using this technique have relatively narrow distribution of chain lengths and may be described as "model" networks.¹¹

In a typical experiment, rectangular strips of the sample (10 cm by 1 cm) were clamped at two ends and subjected to uniaxial tension. The spacing between the sensors was 2 cm. After stretching the sample by the desired amount and allowing about 15 min for relaxation, the level of stress and strain in the network was measured very accurately. A transverse pulse was generated, and the speed was determined from the recorded data. The speed in a polymer network was measured as a function of the strain ($\alpha = L/L_0$) for samples with different molecular weights. The dependence of speed on the degree of cross-linking was studied. For one of the PDMS samples ($M_n = 30\,200$ g/mol), the speed of the pulse was measured for the polymer with different filler concentrations. Effects of swelling were also studied. Finally, we estimated structural parameters of the networks such as M_c and M_e from the pulse propagation measurements using the theoretical framework outlined earlier. All the experiments reported here measured shear wave propagation. The distances between the measurement points and the edges of the sample were large enough to eliminate errors that would result from the finite shape of the sample.

IV. Results and Discussion

IV.1. Pulse Velocity as a Function of Strain. The speed of the pulse was measured for eight PDMS networks with number-averaged molecular weights from 800 to 30 200 g/mol. We stretched the low molecular weight networks to values of $\alpha = 1.35$. For the higher molecular weight networks, we were able to measure up to $\alpha = 2.0$. The speed of the pulse is plotted as a function of the extension ratio, α , as shown in Figure 3a for a network with molecular weight of 1600 g/mol. For the lower molecular weight samples, the increase is linear as predicted by the theoretical framework (see eq 10). For the higher molecular weight samples, the speed increases linearly up to values of α about 1.5 and then increases more sharply (see Figure

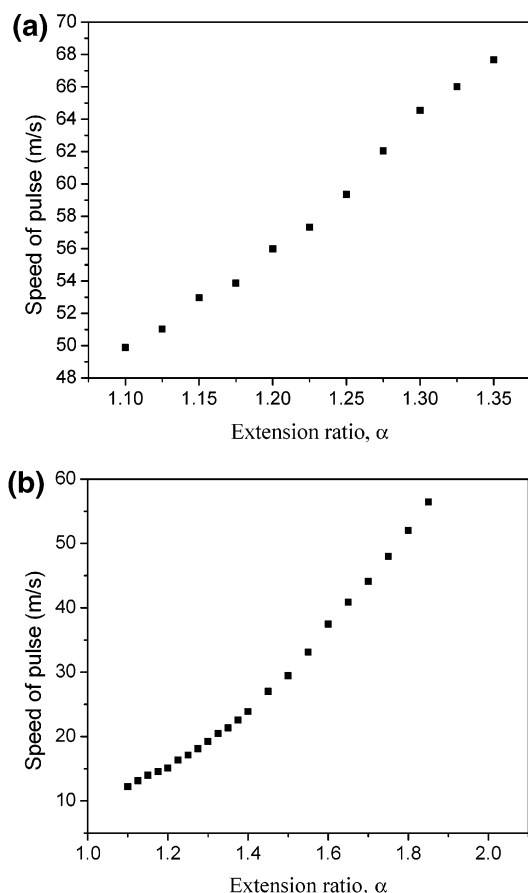


Figure 3. (a) Speed of the pulse is plotted as a function of the extension ratio for $M_n = 1600$ g/mol. (b) Speed of the pulse is plotted as a function of the extension ratio for $M_n = 30\,200$ g/mol.

3b). As the network is subjected to increasing strains, the instantaneous modulus increases because the chains are stretched out along the direction of deformation and causes a stiffening effect or strain hardening. The pulse can then propagate faster along the chains with increasing strain. In section II.3, for a network with $M_n = 10\,000$ g/mol, the lower bound for the pulse velocity in an unstretched network was predicted to be 20 m/s. From our measurements, we obtained the speed in an unstretched PDMS network with $M_n = 17\,600$ g/mol to be 15 m/s. The speed was 24 m/s for a network with $M_n = 6700$ g/mol. For high molecular weight networks under uniaxial tension, the slope of the speed vs extension ratio curve is much smaller at lower values of α . Since considerable numbers of chain entanglements are present in these networks, the increase in speed due to the stretching of chains will occur at higher values of α . At low values of the extension ratio, our data suggest that although the chains are uncoiling, they may not be stretched enough to contribute to an increase in the modulus.

IV.2. Molecular Weight Dependence. The pulse velocity in PDMS networks is expected to depend on the average molecular weight between cross-links according to the relationship predicted by eq 10. In general, the speed of the pulse is expected to decrease with increasing M_c . The behavior observed from our measurements is summarized in Figure 4 at an extension ratio of $\alpha = 1.1$. The pulse velocity is found to be strongly dependent on the network chain length. The speed decreased by 80% from a value of 67 m/s for $M_c = 800$ g/mol to a value

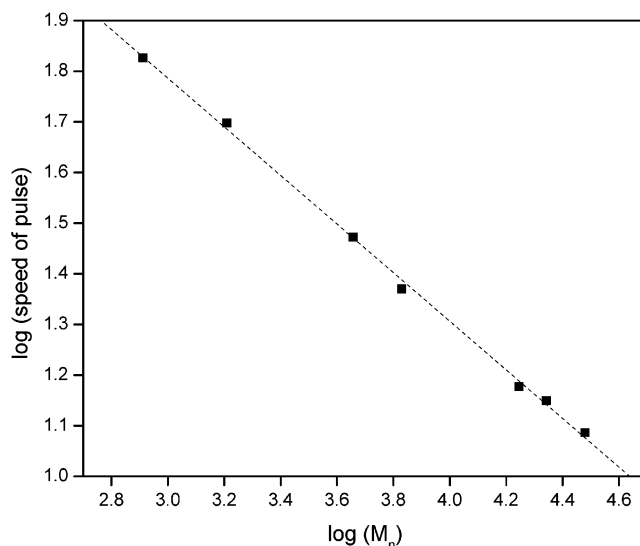


Figure 4. A log-log plot of pulse velocity as a function of reciprocal of M_n for end-linked PDMS at extension ratio, $\alpha = 1.1$.

of 12 m/s for $M_c = 30\,200$ g/mol at $\alpha = 1.1$. The pulse speed decreases sharply with increasing molecular weight for the highly cross-linked networks and becomes constant for molecular weights around 8000–12 000. The square of the pulse velocity is predicted to be linearly proportional to the reciprocal of M_c (see eq 10). The theory suggests a $\log(\text{pulse speed})$ vs $\log(M_c)$ plot will show a slope of -0.5 . Results from our measurements are shown in Figure 4 for the same extension ratios of $\alpha = 1.1$. From experimentally measured pulse speeds, we obtained the slopes to have values of -0.48 ± 0.06 . This demonstrates that at these low extension ratios the affine model predicts network behavior remarkably well. This also shows that this technique will be a useful probe for network behavior because of its sensitivity to network chain length.

IV.3. Effect of Fillers. Amorphous fused silica was used as a filler to prepare networks ($M_c = 30\,200$ g/mol) with 0, 10, 20, and 40% filler. The filler was mixed in uniformly with the PDMS fluid during network preparation. In this case, the filler does not react chemically but is dispersed uniformly through the material. The pulse velocity is measured for these four networks as a function of strain and is shown in Figure 5.

The pulse velocity increases with increasing filler content. This is a direct effect of the increase in the modulus of the network. The velocity increases by about 35% at $\alpha = 1.1$ to almost 200% for $\alpha = 2.0$, comparing a network with no filler to a network with 40% filler. However, no quantitative analysis has been attempted to relate the change in pulse velocity to the amount of filler in the network.

IV.4. Determination of Network Structural Parameters. We have combined molecular models with the theory of elastic wave propagation in order to estimate the microscopic structural parameters of polymer networks from our measurements of pulse velocity. The apparatus can be calibrated using networks of known structural parameters measured independently from GPC and stress-strain experiments.

For uniaxial tension, the expression for the transverse pulse in eq 10 reduces to

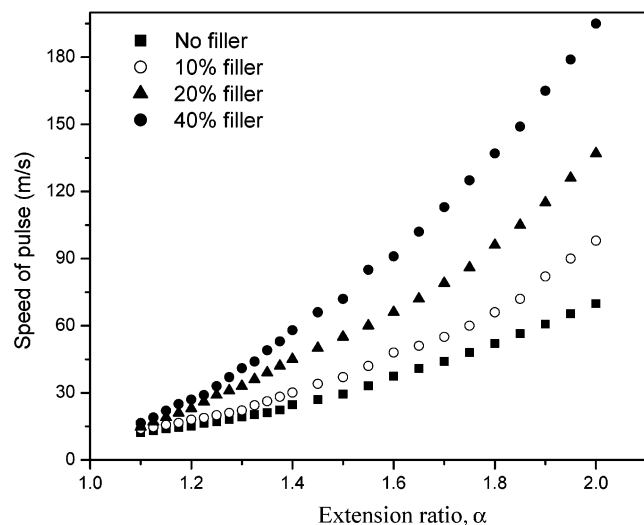


Figure 5. Effect of fillers on pulse velocity in end-linked PDMS networks. The plots show the pulse velocity in networks with 0, 10, 20, and 40% fillers. The speed is shown to be strongly dependent on the level of imposed strain.

$$\rho \frac{U_{12}^2}{\lambda^2} = [f^*]$$

$$\text{where } [f^*] = \frac{fV_2^{1/3}}{A_0(\alpha - \alpha^{-2})} = \text{reduced modulus} \quad (13)$$

where f = force acting along the extension axis measured by the load cell and A_0 = cross-sectional area of the undeformed, dry sample. The reduced modulus $[f^*]$ can be determined from stress-strain measurements, which were carried out at the strain levels where the pulse was generated. Plotting the two sides of the equation for a highly cross-linked network ($M_n = 4500$ g/mol from gel permeation chromatography measurements of network precursor chains), we obtain the curves in Figure 6a. Extrapolating the two curves to zero strain, we can calculate M_c from the y -intercepts using the equation

$$[f^*] = \left(1 - \frac{2}{\phi}\right) \frac{\rho RT}{M_c} \quad (14)$$

We obtain $M_c = 4700$ and 5400 g/mol from the pulse propagation and the reduced modulus curves, respectively.

The value for M_c obtained from the reduced force extrapolated to the $\alpha = 1$ limit of 0.22 N/mm² which corresponds to $M_c = 5400$ g/mol. For the pulse experiments, we obtained an M_c value of 4700 g/mol when a straight line was fitted to all of the data points and extrapolated to $\alpha = 1$. However, extrapolating the straight line through data points for $\alpha^{-1} > 0.8$ gave a value of approximately $M_c = 5400$ g/mol, identical to the limit obtained from reduced force experiments. Within experimental accuracy, we can state that for short chain networks the pulse and stress-strain experiments yield identical results. For finite degrees of deformation, however, the M_c values from pulse experiments were found to be somewhat lower than the M_c values from the plot of the reduced force. In the latter case, it is the equilibrium modulus which is being used to determine the molecular weight. At these low-frequency pulse propagation measurements, although

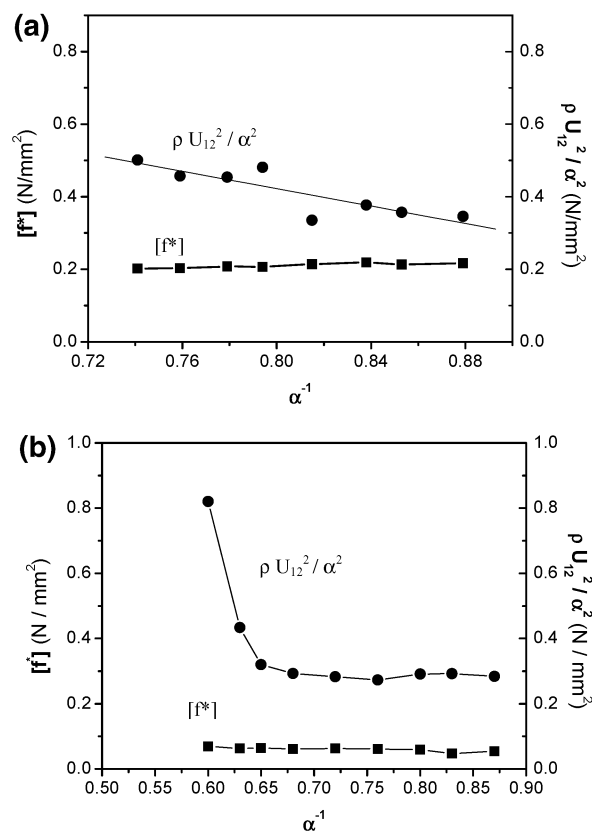


Figure 6. Data obtained from transverse pulse propagation measurements in PDMS networks. Reduced modulus $[f^*]$ and $\rho U_{12}^2/\alpha^2$ have been plotted as a function of the inverse extension ratio (α^{-1}). (a) $M_n = 4500$ g/mol; (b) $M_n = 27\,400$ g/mol.

the modulus is of the same order as the equilibrium case, it will be higher because the propagating wave front will experience a higher modulus due to the presence of chains that are not completely relaxed. The characteristic relaxation times of the samples with high M_c were on the order of milliseconds, although they have not been characterized in detail.

The behavior of a high molecular weight siloxane network (low cross-link density) such as $M_n = 27\,400$ g/mol shows remarkably different behavior (see Figure 6b). The two curves do not converge as we approach zero strain. For this high molecular weight siloxane, we obtain $M_c = 27\,200$ g/mol from the reduced modulus plot. The intercept from the pulse propagation data yields 8500 g/mol, which is in the range of the average weight of the chain between entanglements (M_e) for poly(dimethylsiloxanes).^{16,23} The estimates of entanglement molecular weights sometimes vary greatly, and comparison at this stage is only semiquantitative. The factors affecting the amount of extractables and molecular parameters of the network have been discussed in detail elsewhere.¹¹ The satisfactory agreement of the calculated M_c 's using eq 14 and the molecular weights of the precursor chains from GPC indicates that the reactions were near to completion in all cases. This was verified for all the samples.

This difference in behavior between the low and high molecular weight networks is also seen in the other PDMS samples. A possible explanation for this is the role of entanglements in the high molecular weight networks ($M_c \gg M_e$). In the low molecular weight sample ($M_c \ll M_e$), the chains between cross-links determine

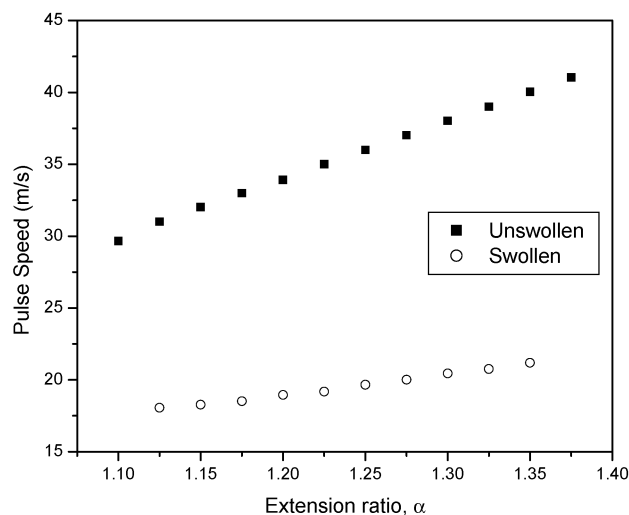


Figure 7. Speed of the pulse is plotted as a function of the extension ratio for $M_n = 4500$ g/mol in the dry and swollen (volume fraction = 0.8) states.

the speed of propagation. On the other hand, entanglement effects are much more prominent in the networks with $M_n = 17\,600$ and higher, where the chain lengths between entanglement points are much shorter than the chains between cross-links. The propagation of the pulse may then be governed by the parameter M_e rather than M_c . Also, in contrast with the low molecular weight networks, the pulse propagation data for the higher molecular weight networks show a sharp upturn at relatively low values of strain. Since this is neither due to limited chain extensibility nor due to strain-induced crystallization, this needs further investigation.

IV.5. Effect of Swelling. In the unswollen or dry state, the wave front that sweeps the sample sees the entanglements as well as the cross-links, and therefore the modulus resulting from pulse propagation would contain effects from entanglements in addition to the equilibrium elasticity of the network. Indeed, as shown above, the moduli obtained in this manner turned out to be larger than the results of static experiments. In this section we report results from swollen networks. These experiments were carried out on networks with molecular weights of 4500 and 27 400 g/mol at polymer volume fractions of 0.9 and 0.8 in order to probe how the modulus changes with swelling. Dodecane was used as the swelling agent for the PDMS networks.

The speed in the swollen network was lower than the speed in the dry network at the same extension ratio. This is shown in Figure 7 for the network with $M_n = 4500$ g/mol. Figure 8 shows the modulus values obtained from both sides of eq 14 for both networks with volume fraction of 0.8. The modulus values obtained from the pulse propagation data on the swollen networks are closer to the equilibrium values than the modulus values obtained from the unswollen networks. This difference is more significant for the higher molecular weight network. The values of M_c calculated from the swollen data compare reasonably well with the GPC measurements of molecular weight.

Neutron spin-echo experiments of Ewen and Richter²² have shown that the junctions in PDMS networks move diffusively. According to these experimental results, the relaxation time for a junction moving in a sphere of ca. 60 Å is about 1 ns. A sharp pulse front traveling at a speed of 12 m/s, for example, would traverse this region

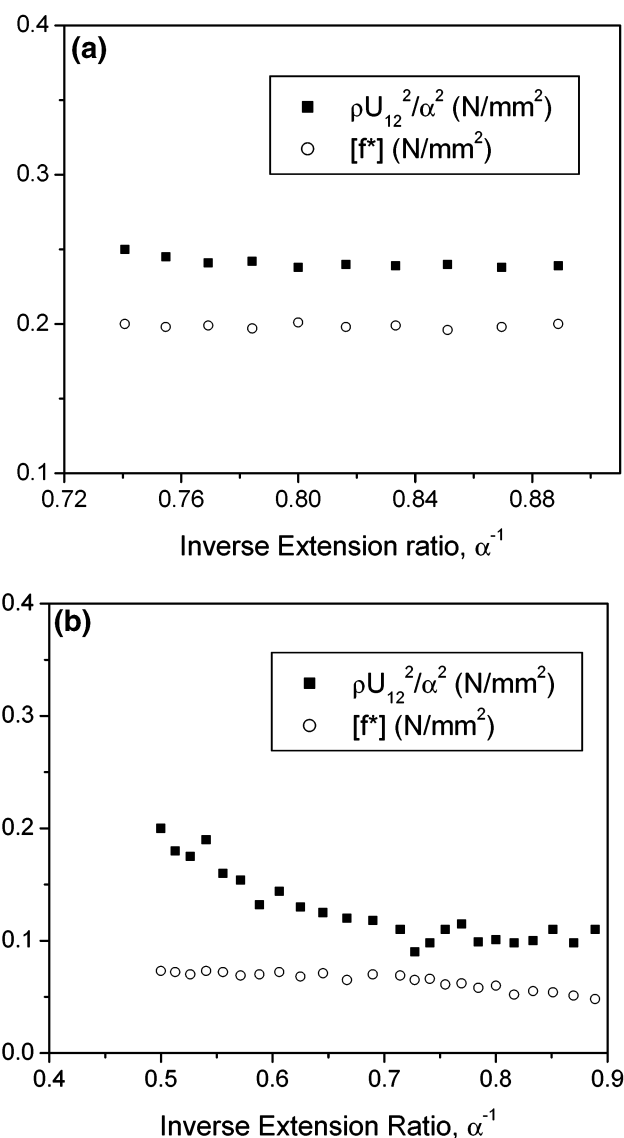


Figure 8. Data obtained from transverse pulse propagation measurements in PDMS networks. Reduced modulus $[f^*]$ and $\rho U_{12}^2/\alpha^2$ have been plotted as a function of the inverse extension ratio (α^{-1}). (a) $M_n = 4500$ g/mol with polymer volume fraction = 0.8; (b) $M_n = 27\,400$ g/mol with polymer volume fraction = 0.8.

in about 0.5 ns, which is of the same order of magnitude of the relaxation time of the junction. When the network is swollen, however, the relaxation time of the junction decreases by several orders of magnitude. Thus, the pulse will see only equilibrium elasticity in moving through swollen samples.

V. Summary

From our measurements of transverse pulse velocity, we were able to determine the average molecular weights of the networks (M_c and M_e), employing elementary molecular models of networks. The pulse velocity was shown to be strongly dependent on deformation, cross-link density, and fillers.

Using the apparatus reported here, we show that transverse pulse propagation measurements in uniaxially stretched PDMS networks can be made conveniently and reproducibly. This is a fast, noninvasive method and can be used for characterizing other polymer networks. It can be used to probe an elastomer that

is being deformed or even adapted to provide a Quality Control tool for a manufacturing process. Our results indicate that for high molecular weight networks entanglements arising from molecular intertwining of chains play a major role in pulse propagation. By establishing the regimes in which elastic behavior will hold true for these networks, the proposed theoretical treatment can be employed to determine M_c and M_e . Under various conditions depending on the relaxation times, the amount of solvent in the network, etc., there may be some viscoelastic losses in these materials (which can be estimated from the reduction in peak amplitude and peak broadening effects). In these regimes, the propagating pulse will see a time varying environment where the chains are still responding to the disturbance. The measured pulse speeds in this case will show different behavior from the predicted ones.

We chose to use poly(dimethylsiloxane) networks for our experiments since it is possible to synthesize model networks using these molecules. This has allowed us to estimate the accuracy of our measurements and to employ the theoretical framework outlined. The experimental method outlined here can be used for any elastomer and therefore holds the promise of applications to other systems in the future.

Acknowledgment. We acknowledge helpful discussions with Alan Gent, V. Sudhindra, and Sathish Sukumaran. We also acknowledge the financial support provided by the National Science Foundation through Grant DMR-0075198 (Polymers Program, Division of Materials Research) and by the Dow Corning Corp.

References and Notes

- (1) Hartmann, B. In *Physical Properties of Polymers Handbook*; Mark, J. E., Ed.; American Institute of Physics Press: Woodbury, NY, 1996; Chapter 49.
- (2) Hartmann, B. In *Methods of Experimental Physics*; Fava, R. A., Ed.; Academic Press: New York, 1980; Vol. 16, Part C.
- (3) Gent, A. N.; Marteny, P. *J. Appl. Phys.* **1982**, *53*, 6069.
- (4) Mark, J. E.; Sullivan, J. L. *J. Chem. Phys.* **1977**, *66*, 1006.
- (5) Truesdell, C. *Arch. Rational Mech. Anal.* **1961**, *8*, 263.
- (6) Toupin, R. A.; Bernstein, B. *J. Acoust. Soc. Am.* **1961**, *33*, 216.
- (7) Hayes, M.; Rivlin, R. S. *Arch. Rational Mech. Anal.* **1961**, *8*, 15.
- (8) Chen, P. J. *Arch. Rational Mech. Anal.* **1968**, *31*, 228.
- (9) Varley, E. *Arch. Rational Mech. Anal.* **1965**, *19*, 215.
- (10) For a review of the terminology, refer to: Truesdell, C. F.; Toupin, R. A. *Handbuch der Physik*; Flugge Berlin-Gottingen-Heidelberg, Ed.; Springer: Berlin, 1960; Vol. 3/1, p 225.
- (11) Erman, B.; Mark, J. E. *Structures and Properties of Rubber-like Networks*; Oxford University Press: New York, 1997.
- (12) Flory, P. J. *Proc. R. Soc. London, Ser. A* **1976**, *351*, 351.
- (13) Edwards, S. F. *Polymer* **1986**, *27*, 483.
- (14) Flory, P. J.; Erman, B. *Macromolecules* **1982**, *15*, 800.
- (15) Erman, B.; Monnerie, L. *Macromolecules* **1989**, *22*, 3342.
- (16) Graessley, W. W. In *Advances in Polymer Science*; Springer-Verlag: Berlin, 1974; Vol. 16.
- (17) Noordermeer, J. W. M.; Ferry, J. D. *J. Polym. Sci., Polym. Phys. Ed.* **1976**, *14*, 509.
- (18) Thirion, P.; Monnerie, L. *J. Polym. Sci., Polym. Phys. Ed.* **1986**, *24*, 2307.
- (19) Erman, B. Unpublished results.
- (20) Ozkul, M. H.; Onaran, K.; Erman, B. *J. Polym. Sci., Polym. Phys. Ed.* **1990**, *28*, 1781.
- (21) *Polymer Handbook*, 4th ed.; Brandrup, J., Immergut, E. H., Grulke, E. A., Eds.; Wiley-Interscience: New York, 1999.
- (22) Ewen, B.; Richter, D. In *Elastomeric Polymer Networks*; Mark, J. E., Erman, B., Eds.; Prentice Hall Polymer Science and Engineering Series; Prentice Hall: Englewood Cliffs, NJ, 1992.
- (23) *Physical Properties of Polymers Handbook*; Mark, J. E., Ed.; American Institute of Physics Press: Woodbury, NY, 1996; Chapter 24.

MA030168F